Optical Phased Array Chip-based Free-Space QKD Experiment Using Compact Quantum Photonics Modules

Minchul Kim,[1,2,†] Junsang Oh,[1] Byung-Seok Choi,[1] Joong-Seon Choe,[1] Ju Hee Baek,[1] Chun Ju Youn,[1] Hyo-Hoon Park,[2] Hamza Kurt,[2] and Hoon Kim[2,*]

[1] *Electronics and Telecommunications Research Institute (ETRI), Daejeon 34129, South Korea*
[2] *Korea Advanced Institute of Science and Technology (KAIST), Daejeon 34141, South Korea*

[†] *minchul.kim@etri.re.kr,* [*] *hoonkim@kaist.ac.kr*

Abstract: We demonstrate the first free-space QKD experiment using an optical phased array chip for compact, fully integrated, and mobile free-space QKD systems. We achieve 1% QBER for a couple of beam steering conditions.

1. Introduction

Quantum key distribution (QKD) offers unconditional security based on fundamental physical laws and is regarded as a next-generation secure communication technology. Among various approaches, free-space QKD has been actively investigated for its potential applications in long-distance global QKD networks and mobile platforms [1–4]. Recently, the expanding use of compact mobile platforms such as autonomous vehicles and drones has driven increasing interest in short-to medium-range free-space QKD systems capable of ensuring secure communication in such environments [5–8].

An effective way to realize compact QKD systems is to employ photonic integrated circuits (PICs) instead of conventional bulk-optic components. Similar to fiber-based QKD systems, recent studies have demonstrated chip-based free-space QKD implementations [9–12]. However, previous compact free-space QKD systems were often limited by bulky or incomplete pointing, acquisition, and tracking (PAT) implementations. These limitations can be overcome by utilizing optical phased array (OPA) technology. An OPA enables rapid beam steering without any mechanically moving parts by precisely controlling the phase of optical waves emitted from multiple adjacent radiators. OPA devices are inherently compact, fast, robust, and suitable for mass production, making them attractive for free-space optical (FSO) communication applications [13, 14]. Nevertheless, research exploiting OPA technology in quantum optics and QKD systems remains very limited [15].

In this work, we report, to the best of our knowledge, the first implementation of a free-space QKD system employing an OPA chip. A 16-channel OPA chip fabricated using CMOS-compatible silicon photonics platform was used for QKD experiment. Phase-encoded BB84 signals generated by a PIC-based QKD transmitter module were emitted through the OPA and detected at a receiver which also employed a PIC-based module. Furthermore, we confirmed QKD operation when the output quantum signal was steered using the OPA. The system achieved a QBER of about 1% for all bases, demonstrating the feasibility of OPA-based free-space QKD.

2. Optical Phased Array Module

The silicon-photonic OPA chip used in this work consists of an input coupler, a splitter array, a phase shifter array, and an output radiator array. Fig. 1(a) shows the schematic of the fabricated OPA chip. A grating coupler was employed as the input coupler, and a four-stage multimode interferometer MMI splitter array was designed to divide the optical signal into 16 channels. Each divided signal was guided to a phase shifter, which compensates for phase differences in the waveguide and precisely controls the relative phase so that the light emitted from the radiator array is directed toward the desired angle. The carrier-injection p–i–n phase shifter was selected for high-speed phase modulation and low crosstalk between adjacent channels. The achievable beam-steering range and divergence are determined by the radiator spacing, width, and length, which were 1 μm, 31 μm, and 19 μm, respectively. The total size of the designed OPA device was only 2.3 mm × 0.6 mm.

The OPA chip was fabricated on an 8-inch silicon-on-insulator (SOI) wafer using a KrF laser–based, CMOS-compatible process. The beam steering range of the fabricated chip reached $\pm 14^\circ$, as shown in Fig. 1(b) and 1(c). The fabricated chip was diced and mounted on a dedicated printed circuit board (PCB), and the electrical pads were wire-bonded, as shown in Fig. 1(c). To enable optical input without a fiber alignment stage, a fiber block

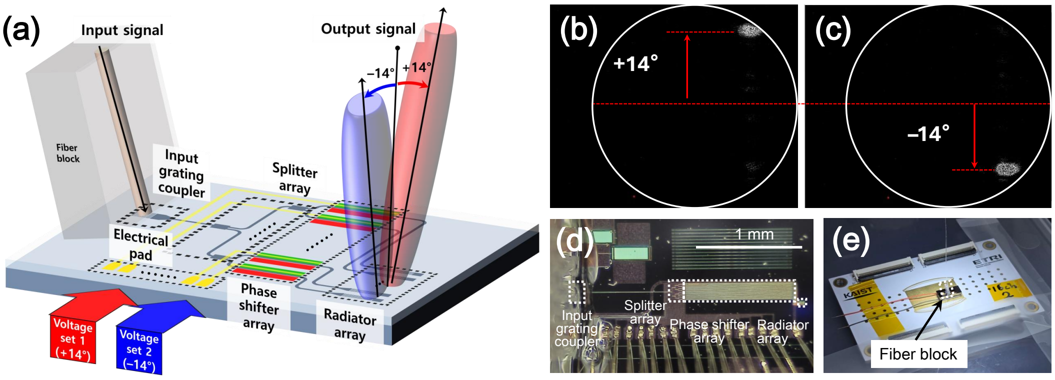

Fig. 1. (a) Schematic of the 16-channel optical phased array (OPA) chip. The output beam is steered to $+14^\circ$ and -14° when voltage sets 1 and 2 are applied, respectively. (b), (c) Measured far-field beam-profile images showing optical beams steered to $+14^\circ$ and -14°, respectively. (d) Microscope image of the fabricated and wire-bonded OPA chip. (e) Photograph of the packaged OPA module with a fiber block attached for optical input.

was attached to the input grating coupler, as illustrated in Fig. 1(d). The final insertion loss of the assembled OPA module was measured to be 18.1 dB.

3. Experimental Setup and Results

To evaluate the QKD performance, a free-space testbed was established with a propagation distance of approximately 0.7 m, as shown in Fig. 2(a). The quantum signal was generated from a PIC-based QKD transmitter (Tx) module integrating a laser diode, an asymmetric Mach–Zehnder–type delay line interferometer, two-stage variable optical attenuators, and a phase modulator. The generated optical signal passed through a polarization controller and was then injected into the OPA module, where the beam direction was controlled by a voltage set applied to the OPA. Two experimental conditions were tested to verify the QKD operation under different OPA steering angles. In Tests #1 and #2, the OPA was rotated by $\pm 14^\circ$, and the emitted quantum beam was electronically steered to $\mp 14^\circ$ using voltage sets 1 and 2, respectively. The measured free-space coupling loss at the receiver-side fiber collimator were 12.1 dB and 13.9 dB. The coupling losses were attributed to beam shape differences, alignment, and the limited focal adjustment range of the collimating optics. After the transmitted quantum signal was collected at the receiver, it passed through a polarization controller and a phase modulator for basis selection. The signal was then injected into the QKD receiver (Rx) module, which consisted of a delay line interferometer chip. The interfered optical signals were split accordingly and detected by single-photon detectors (SPDs). The electrical clicks generated by the SPDs were recorded using a data acquisition (DAQ) device and analyzed on a computer. The detection efficiencies of SPD-0 and SPD-1 were both 10%, and the dark count rates were 79 counts/s and 105 counts/s, respectively.

The measurement results for Test #1 are summarized in Fig. 2(b) and 2(c). When the transmitted quantum states were $|0\rangle$ and $|1\rangle$, and the receiver measured in the Z basis, the QBERs were 1.3% and 0.9%. The count rates for the SPDs were 40,806 and 520 counts/s for the $|0\rangle$ state, and 418 and 45,215 counts/s for the $|1\rangle$ state, respectively. When the transmitted states were $|+\rangle$ and $|-\rangle$, and the receiver measured in the X basis, the QBERs were 1.0% and 0.6%. The count rates for the SPDs were 41,630 and 414 counts/s for the $|+\rangle$ state, and 968 and 47,828 counts/s for the $|-\rangle$ state, respectively. The results for Test #2 are shown in Fig. 2(d) and 2(e). For the $|0\rangle$ and $|1\rangle$ states measured in the Z basis, the QBERs were 1.4% and 0.8%. The count rates for the SPDs were 27,713 and 390 counts/s for the $|0\rangle$ state, and 33,793 and 288 counts/s for the $|1\rangle$ state, respectively. For the $|+\rangle$ and $|-\rangle$ states measured in the X basis, the QBERs were 1.4% and 1.3%. The count rates for the SPDs were 28,355 and 410 counts/s for the $|+\rangle$ state, and 413 and 30,600 counts/s for the $|-\rangle$ state, respectively. These results confirm that QKD operation is maintained even when the optical beam direction is dynamically controlled by the OPA.

4. Conclusions

In this work, we demonstrated the first free-space QKD system employing a compact OPA chip. Stable quantum signal transmission and a low quantum bit error rate (QBER) of about 1% were achieved under dynamic beam steering of $\pm 14^\circ$, without any mechanically moving parts. By incorporating PIC-based QKD modules and OPA module, this study demonstrates the feasibility of realizing the PAT functionality for QKD on a photonic integrated chip, paving the way for fully integrated on-chip free-space QKD transmitters. As the phase-encoded BB84

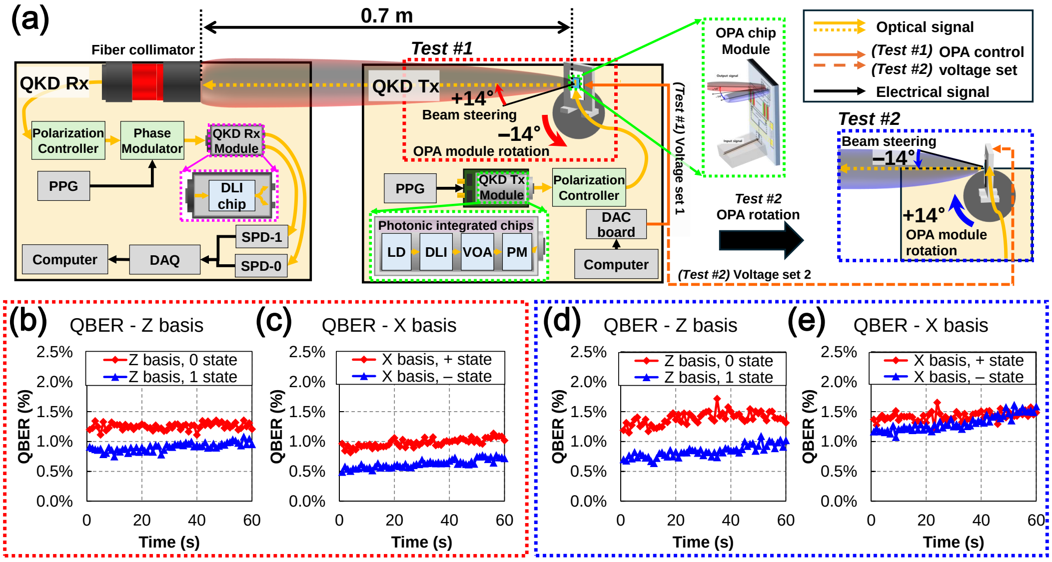

Fig. 2. (a) Photograph and schematic of the free-space QKD testbed using PIC-based QKD transmitter (Tx) and receiver (Rx) modules with the OPA module. The Tx module integrates a laser diode (LD), delay line interferometer (DLI), variable optical attenuator (VOA), and phase modulator (PM) chips, while the Rx module includes a DLI chip. Test #1 and Test #2 correspond to OPA module rotations of −14° with beam steering of +14°, and +14° with beam steering of −14°, respectively. (b), (c) Measured quantum bit error rates (QBERs) for Test #1 in the Z and X bases. (d), (e) QBERs for Test #2 in the Z and X bases, respectively.

protocol is widely employed in fiber-based QKD systems, the proposed approach enables seamless extension of fiber-based QKD networks to mobile free-space links without additional QKD transmitters or relay nodes.

5. Acknowledgements

This work was supported by the IITP grant funded by the Korea government (RS-2019-II190005, RS-2022-II221014, RS-2024-00398716, RS-2025-02218080). This work was also supported by the NRF grant funded by the Korea government (No. RS-2024-00439005).

References

1. S. Nauerth *et al.*, "Air-to-ground quantum communication," *Nat. Photonics* **7**, 382–386 (2013).
2. S.-K. Liao *et al.*, "Satellite-to-ground quantum key distribution," *Nature* **549**, 43–47 (2017).
3. C. J. Pugh *et al.*, "Airborne demonstration of a quantum key distribution receiver payload," *Quantum Sci. Technol.* **2**, 024009 (2017).
4. H. Takenaka *et al.*, "Satellite-to-ground quantum-limited communication using a 50-kg-class microsatellite," *Nat. Photonics* **11**, 502–508 (2017).
5. H. Chun *et al.*, "Handheld free-space quantum key distribution with dynamic motion compensation," *Opt. Express* **25**, 6784–6795 (2017).
6. G. Vest *et al.*, "Quantum key distribution with a hand-held sender unit," *Phys. Rev. Appl.* **18**, 024067 (2022).
7. A. Conrad *et al.*, "Drone-based quantum key distribution (QKD)," in *Free-Space Laser Communications XXXIII*, Proc. SPIE **11678**, 116780N (2021).
8. X.-H. Tian *et al.*, "Experimental demonstration of drone-based quantum key distribution," *Phys. Rev. Lett.* **133**, 200801 (2024).
9. H. Ko *et al.*, "Daylight operation of a high-speed free-space quantum key distribution using silica-based integration chip and micro-optics-based module," in *Optical Fiber Communications Conference and Exhibition (OFC)* (IEEE, 2019), pp. 1–3.
10. M. Avesani *et al.*, "Full-daylight quantum-key-distribution at 1550 nm enabled by integrated silicon photonics," *npj Quantum Inf.* **7**, 93 (2021).
11. K. Lim *et al.*, "Photonic integrated chip-based reference-frame-independent quantum key distribution transmitter," in *Optical Fiber Communications Conference and Exhibition (OFC)* (IEEE, 2025), pp. 1–3.
12. F. Honz *et al.*, "World's first monolithic SiGe QKD transmitter chip," in *Optical Fiber Communication Conference (OFC)* (Optica Publishing Group, 2025), paper Th4A.3.
13. H.-W. Rhee *et al.*, "32 Gbps data transmission with 2D beam-steering using a silicon optical phased array," *IEEE Photon. Technol. Lett.* **32**, 803–806 (2020).
14. J.-Y. Kim *et al.*, "Demonstration of high-speed wireless data transmission using passive silica optical phased array," in *Free-Space Laser Communications XXXV*, Proc. SPIE **12413**, 124130V (2023).
15. V. Gurses *et al.*, "An on-chip phased array for non-classical light," *Nat. Commun.* **16**, 6849 (2025).